Sensors & Actuators: B. Chemical 355 (2022) 131326

Contents lists available at ScienceDirect

Sensors and Actuators: B. Chemical

journal homepage: www.elsevier.com/locate/snb

A highly sensitive and flexible photonic crystal oxygen sensor

Sai Chen [a], Qun Ren [b], Ke Zhang [a,*], Wei E.I. Sha [c], Tingting Hao [a], Hongbo Xu [a], Jiupeng Zhao [a,*], Yao Li [d,*]

[a] MIIT Key Laboratory of Critical Materials Technology for New Energy Conversion and Storage, School of Chemistry and Chemical Engineering, Harbin Institute of Technology, Harbin 150001, China
[b] School of Electrical and Information Engineering, Tianjin University, Tianjin 300072, China
[c] State Key Laboratory of Modern Optical Instrumentation, College of Information Science and Electronic Engineering, Zhejiang University, Hangzhou 310027, China
[d] Center for Composite Materials, Harbin Institute of Technology, Harbin 150001, China

ARTICLE INFO

Keywords:
Oxygen sensor
Photonic crystals
High sensitivity
Fluorescence enhancement effect

ABSTRACT

Oxygen sensing attracts high research interest because it is applicable to early diagnosis and health monitoring. Herein, based on photonic crystals (PCs), a novel fluorescence enhancement effect (FEE) was explored to achieve highly sensitive and accurate oxygen detection. A flexible oxygen sensor was fabricated from heterogeneous polydimethylsiloxane (PDMS) and polystyrene (PS) PCs embedded with platinum(II) octaethylporphyrin (PtOEP) oxygen-sensitive dye. Two different fluorophore incorporation (PtOEP-in and PtOEP-out) PCs were compared in terms of their FEE and oxygen-sensing performance. Simultaneously, photoluminescence enhancement was experimentally and theoretically examined and was determined to be the main factor in improving the performance of the oxygen sensor. In particular, the optimized PC oxygen sensor showed a 12-fold higher PL intensity than PS microspheres (control group). Moreover, the optimized sensor demonstrated high sensitivity to oxygen, with excellent accuracy, photostability and flexibility. This work is expected to provide a universal route to design flexible PC sensors for health monitoring through fluorescent ultratrace detection.

1. Introduction

Oxygen is closely related to the metabolism of all living creatures. With the rapid development of early medical diagnosis, numerous diseases, such as cancer [1], tumor [2] and burns [3], can be monitored by oxygen sensing. Compared with Clark electrodes [4], optical oxygen sensors based on "phosphorescence quenching" have no oxygen consumption and are reversible and noninvasive;[5] however, their sensitivity, signal-to-noise ratio [6] and stability are seriously limited because of the interference of photobleaching and fluorescence signals from the background. Most importantly, mechanical flexibility [7] is urgently needed to validate the sensor's applicability as a flexible oxygen sensor [8], considering that the sensor platforms are most likely to be attached on curved surfaces, or stretched by human skin during operation [9]. To meet these demands, flexible photonic crystals (PCs) have been introduced into oxygen sensors to create a highly sensitive and flexible oxygen sensor based on the FEE principle.

An optical oxygen sensor is mainly based on dynamic quenching of an oxygen-sensitive probe (OSP) in the excited state [10]. Therefore, oxygen sensing mainly depends on the OSP and matrix materials [11] that act as dispersion or support materials in oxygen sensors. In the literature, Wang et al [12]. and Borisov et al [13]. synthesized supramolecular polymer nanoprobes and new dual-emission complexes to improve the performance of oxygen sensors in live-cell imaging. Among the studied OSPs, platinum(II) octaethylporphyrin (PtOEP), with a high quantum yield and a long phosphorescent lifetime, is a promising candidate for OSPs. In addition, many researchers have found that the sensitivity of oxygen sensors can be effectively improved by developing gas diffusion of the support materials. For example, Park et al [14]. and Tian et al [15]. prepared a porous thin film to improve oxygen sensitivity via to the higher gas accessibility provided by porous channels. However, the nonuniform microenvironment of porous thin films usually leads to leakage of the OSP. Therefore, the high sensitivity of oxygen sensors provided by porous structures cannot be guaranteed for a long time. In addition, enhancing the PL intensity of the OSP is an alternative method used to increase the sensitivity of oxygen sensors. Cai et al [16]. and Park et al [17]. developed a highly sensitive oxygen sensor with TiO_2 nanoparticle doping, which substantially enhanced the PL intensity

* Corresponding authors.
E-mail addresses: zhangke@hit.edu.cn (K. Zhang), jpzhao@hit.edu.cn (J. Zhao), yaoli@hit.edu.cn (Y. Li).

https://doi.org/10.1016/j.snb.2021.131326
Received 21 September 2021; Received in revised form 5 December 2021; Accepted 27 December 2021
Available online 29 December 2021

of OSP because of the light scattering effect of nanoparticles [18].

PCs with highly ordered structures [19] can be conveniently fabricated by bottom-up self-assembly of monodisperse microspheres, such as polystyrene (PS) [20], polymethyl methacrylate (PMMA) [21], and silica (SiO_2) [22]. The periodically modulated refractive index opens up a photonic bandgap in PCs [23,24], and brilliant structural colour with anti-photobleaching is realized. Additionally, in view of the angle- and crystal lattice-dependent photonic bandgaps [25], many efforts have been made to apply PCs in the fields of anti-counterfeiting [26], patterning [27], and sensing [28]. In particular, PCs show strong FEE when the photonic bandgap of PCs partially overlaps with the emission peak of dyes [29,30]. PC-facilitated FEE has been used for a variety of dyes, such as cyanine [31], rhodamine [32], and quantum dots [33]. Moreover, light trapping in PCs has been employed to explain the FEE [34], through which dyes in PCs can be repeatedly excited. Recently, FEE has been widely utilized to monitor DNA [35], cocaine [36], metal ions [37], chlorobenzene [38], nucleic acids [39] and other substances [40]. Compared with traditional fluorescence analysis technology, PC-based methods have higher sensitivity and a lower detection limit [41]. However, no highly sensitive PC oxygen sensor with FEE has been reported thus far.

Herein, to improve the flexibility, sensitivity, signal-to-noise ratio, and stability in oxygen sensing, we introduced PCs into an oxygen sensor, and a three-layer heterogeneous flexible PC structure was developed. In the trilayer structure, the top and bottom layers are polydimethylsiloxane (PDMS), which is a hydrophobic polymer with excellent mechanical properties that effectively prevents OSP leakage. The middle layer is the key layer, for which monolithic PCs composed of PS microspheres and PtOEP were prepared. Furthermore, PtOEP-in and PtOEP-out flexible oxygen sensors, which differ based on the position of PtOEP loaded inside PCs (gap or body), were comparatively studied in terms of their FEE and oxygen sensing. Finally, excellent flexibility and oxygen sensing stability were proved by 100 continuous stretches. Thus, the oxygen sensor developed in this study demonstrated high sensitivity, satisfactory stability and excellent flexibility.

2. Experimental section

2.1. Materials

Platinum octaethylporphyrin (PtOEP) was obtained from J&K Chemical Company Limited. Tetrahydrofuran (THF) was purchased from Xilong Chemical Co. Styrene and fluorescein isothiocyanate (FITC) were purchased from Sigma-Aldrich, Inc., and polydimethylsiloxane (PDMS) SYLGARD-184 was purchased from Dow Corning, Inc. Ultrapure water (18.2 $M\Omega \cdot cm^{-1}$) was used directly from a Millipore System (Marlborough, France). All chemicals were used as received without further purification.

2.2. Preparation of two different fluorophore incorporation PCs

PS colloidal suspensions were prepared via a soap-free method [42]. Two different fluorophore incorporation approaches were then used to introduce PtOEP into the PC structure in this study: infiltration (PtOEP-out) and swelling (PtOEP-in).

PtOEP-out: Monolithic PCs were formed from 10 ml of PS microspheres (0.2 wt%) using the evaporation-induced vertical deposition method [43], and then, 20 μl of PtOEP/C_2H_5OH (10^{-3} mol/l) solution was obliquely infiltrated into the PS PCs. These samples were denoted as PtOEP-out PCs.

PtOEP-in: In detail, a certain amount of PtOEP/THF (10^{-3} mol/l) solution was added to a 10 ml PS microsphere suspension. After a period of mixing ranging from 1 h to 2 h, the PtOEP swelling process reached equilibrium. Then, PtOEP-in PCs were prepared by the evaporation-induced vertical deposition method [43].

2.3. Fabrication of a flexible PDMS/PS/PDMS PC oxygen sensor

To obtain a hydrophilic surface, quartz was consecutively cleaned by ultrasonication in ultrapure water, ethanol, and ultrapure water again for 15 min, followed by plasma treatment for 20 min. As shown in Scheme 1, first, a 10:1 (v/v) mixture of PDMS prepolymer and curing agent was deposited dropwise on a quartz substrate, and then, PDMS was also cured by vacuum drying at 60 °C for more than 10 h. PDMS was also hydrophilized using plasma. Monolithic PS PCs were assembled via the evaporation-induced vertical deposition method [43]. After another thin PDMS film was cured on the PS PCs, a flexible PDMS/PS/PDMS PC oxygen sensor was obtained.

2.4. Characterization

The distribution of PtOEP in PS microspheres was observed by transmission electron microscopy (FEI TALOS F200X, America). The surface morphology of PS PC oxygen-sensing films was characterized via field-emission scanning electron microscopy (FE-SEM, SUPRA 55 SAPPHIRE, Carl Zeiss, Germany). Reflection spectra were measured by an optical fibre spectrometer (Ocean Optics Maya 2000 Pro), where both incident and reflected angles were perpendicular to the surface of the sample. The strain cycles were tested using a microcomputer plug force testing machine (MEIKO, Dongwan Guangzhou, China), and the reflection spectra of oxygen-sensing thin films during strain cycles were also obtained using an optical fibre spectrometer. The structural colour in optical images was captured with a phone camera.

Oxygen-sensing properties were measured by a fluorescence spectrometer (LS55, Perkin Elmer, America), which was equipped with a self-regulating nitrogen/oxygen mixture device [44]. Different oxygen contents were controlled by the flow rates of N_2 or O_2 during the testing of oxygen sensing.

3. Results and discussion

3.1. Design, preparation, and characterization of the PC FEE oxygen sensor

To evaluate the effect of particle size of PC on fluorescence enhancement in PC-based sensors, the PC with 241 nm and 250 nm PS microspheres were compared on stopband positions (Fig. S1). Then, a three-layer heterogeneous PC structure was designed for the flexible oxygen sensor (**see the Experimental Section**). As illustrated in Scheme 1, three main procedures were used to prepare the oxygen-sensing thin film. (i) Monodisperse PS microspheres were assembled into monolithic PCs by an evaporation-induced vertical deposition method [43], which is the most feasible and controllable method for bottom-up self-assembly. (ii) The OSP was embedded into PS PCs at two different positions (PtOEP-out by infiltration and PtOEP-in by swelling). (iii) Two thin PDMS films were combined with the above monolithic PS PCs for transfer of the oxygen-sensing thin film. To obtain the FEE, the diameter of PS microspheres forming the PCs was calculated by Bragg's diffraction law (Equation S1).

Field-emission scanning electron microscopy (FE-SEM), high-angle annular dark-field scanning transmission electron microscopy (HAADF-STEM), and energy-dispersive X-ray spectroscopy (EDS) were used to characterize the prepared PS PCs with various PtOEP incorporations. Since PS microspheres change to a loosened structure after swelling, the PS microspheres gradually become a regular hexagon under the influence of squeezing during self-assembly (Fig. S2a-e). However, all PS microspheres still have monodisperses with slightly changed sizes (Fig. S3a-f); the reflection peak of the PS PCs is redshifted, and the corresponding reflectivity of the PS PCs decreases (Fig. S4a and b) because PS fills the air gaps of the PCs. Notably, the thickness of PS PCs is 6.95 μm (Fig. 1a), and an integral circle made of PtOEP is formed at the "under the skin coating" of PS microspheres (Fig. 1b). HAADF-

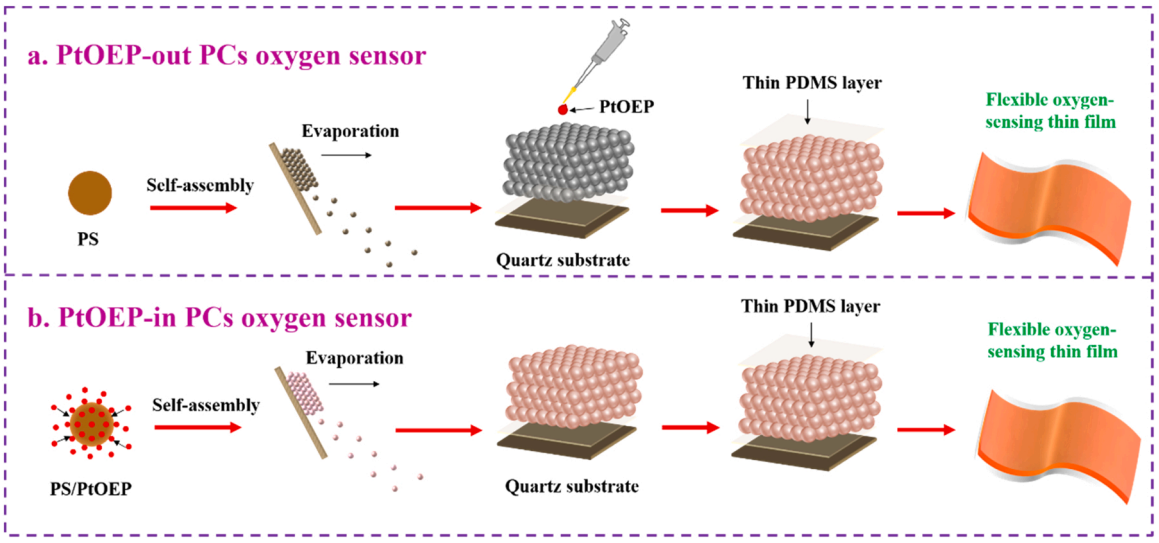

Scheme 1. Schematic for the preparation of PC oxygen sensors by the self-assembly method: (a) PtOEP-out oxygen sensor; (b) PtOEP-in oxygen sensor.

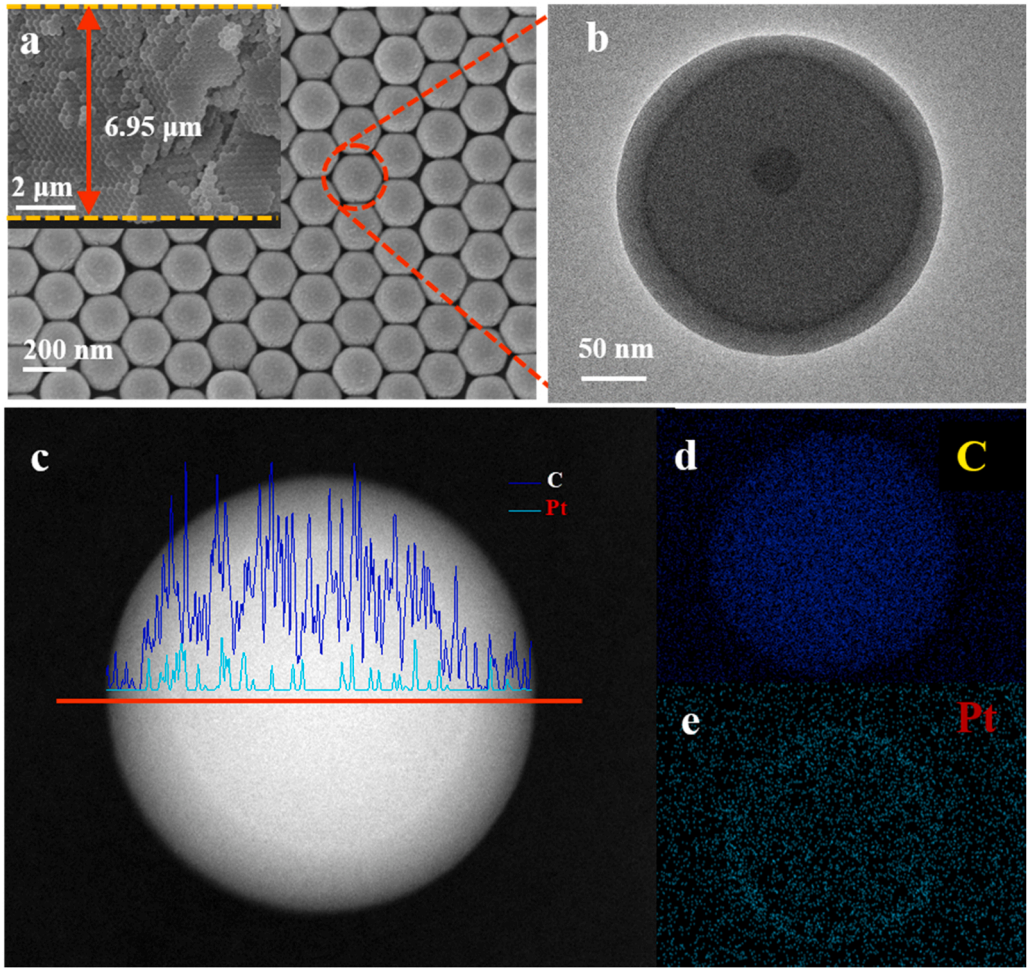

Fig. 1. (a) SEM image of PS PCs with a microsphere diameter of 250 nm; the inset shows a SEM image of the classic PC thickness; (b) TEM image of swelling microspheres; (c) HAADF-STEM image of a microsphere, and EDS image of Pt and C; (d-e) mapping of Pt and C.

STEM and EDS images show that a brighter circle appears inside the PS microspheres. The amount of Pt that exists at the edges is presumed to be more than that inside, which is because PtOEP molecules are primarily physically bound to the PS surface through the entanglement of the polymer chains in the process of swelling (Fig. 1c). Additionally, the mapping of C and Pt shows a complete circle (Fig. 1d and e), demonstrating that PtOEP is evenly distributed inside the PS microspheres.

Two flexible PC FEE oxygen sensors with PtOEP-in and PtOEP-out PCs were prepared by self-assembly, as illustrated in Scheme 1. The reflection spectra of PS/air (PS PCs with air filled in the gap) and PS/PDMS (PS PCs with PDMS filled in the gap), as well as the emission peak of PtOEP, were obtained (Fig. 2**a**), showing that the emission peak of PtOEP partially overlaps with the PS photonic bandgap, which enhances the PL of PtOEP [45]. Notably, the PL intensity of PtOEP-in PCs is better than that of PtOEP-out PCs due to the well-dispersed dye in the spheres and weak self-quenching [46] of the dye in PtOEP-in PCs (Fig. 2**b**).

In addition, the theoretical analysis of the PL enhancement of PtOEP in PCs is discussed. To illuminate the underlying physics of PL enhancement, our theoretical explanation starts from the photon local density of states (LDOS), which is one of the cruxes of luminescence efficiency. For instance, the capacity of the optical modes provided by artificial photonic engineering structures such as PCs could manipulate the electromagnetic field in space and thus intensify the LDOS, which is beneficial for faster spontaneous emission processes and higher PL enhancement. As described in Fig. 3**a and c**, the field distribution (an indicator of LDOS) at the junction between PtOEP-in PS microspheres increases significantly at resonance frequency, resulting in a decreased radiation recombination lifetime and thus enhanced PL. However, due to the lower index difference between PS spheres and surroundings (Fig. 3**b and d**), the near field is scattered in the structures, and the LDOS is weaker. Therefore, the different localization of photons in PtOEP-in PCs provides the reason for greater luminescence in PtOEP-in PCs than in PtOEP-out PCs (Fig. 2**b**). Here, the lattice constants of the unit cell in Fig. 3(**a**, **b**) in the X direction are 250 nm and $250\sqrt{3}$ nm in the Y direction. The refractive indices of the PS spheres and PtOEP simulated in this work were retrieved from previous experimental data [47,48]. The light source for the field distribution is plane waves from 600 nm to 700 nm.

On another level, however, for the PtOEP-out PCs, the radiation is random in space, and the coherence is poor. The high index difference of PtOEP-in PCs gives an approach for radiating toward a particular pattern. The Purcell effect can also explain this phenomenon. As illustrated in Fig. 4, we calculated the Purcell factors with different dipole positions for both the PtOEP-in PCs and PtOEP-out PCs using FDTD numerical simulation. It was found that the Purcell effect depends heavily on the dipole positions. At the junction between PS spheres, the Purcell factor of PtOEP-in PCs can be up to 18 times larger than that of PtOEP-out PCs. When the dipole is positioned far from the exact junction, the enhancement Purcell factor decreases severalfold because there is a low LDOS. The difference in the optical properties comes from the coherence and localization of the optical field. For PtOEP-in PCs, the high index difference contributes to a stronger localization of photons with high radiation toward a particular pattern, which exhibits greater luminescence. For the PtOEP-out PCs, however, the radiation is random in space, and the optical coherence is poor due to the low index difference between PS spheres and PtOEP surroundings. In other words, PtOEP-in PC behaves as a light-trapping optical material with high luminescence efficiency, whereas for PtOEP-out PC, light is almost uniformly distributed in the composite material exhibiting a low photon density of states and divergent field.

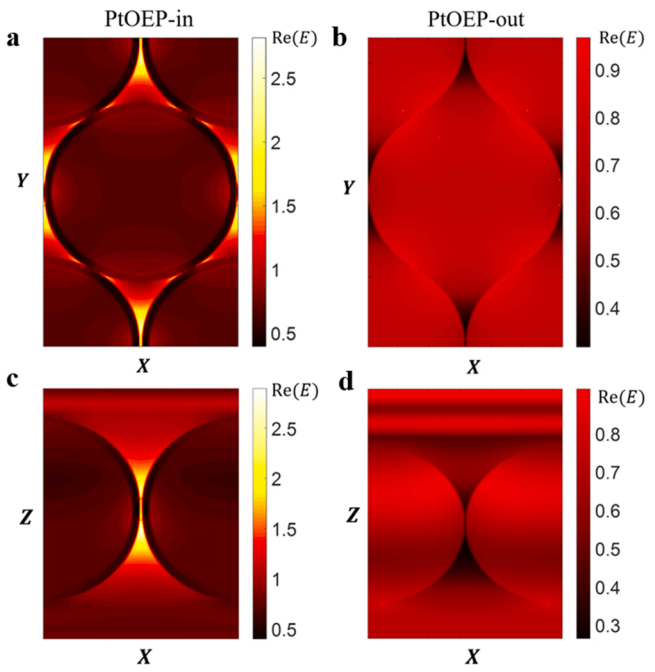

Fig. 3. (a, c) E field profiles at the XOY and XOZ planes of PtOEP-in PCs at resonance; (b, d) E field profiles at the XOY and XOZ planes of PtOEP-out PCs at resonance.

A 12-fold enhancement of PtOEP-in PCs was obtained compared with the control group (disorderly PS microspheres) (Fig. 5), while a 4-fold

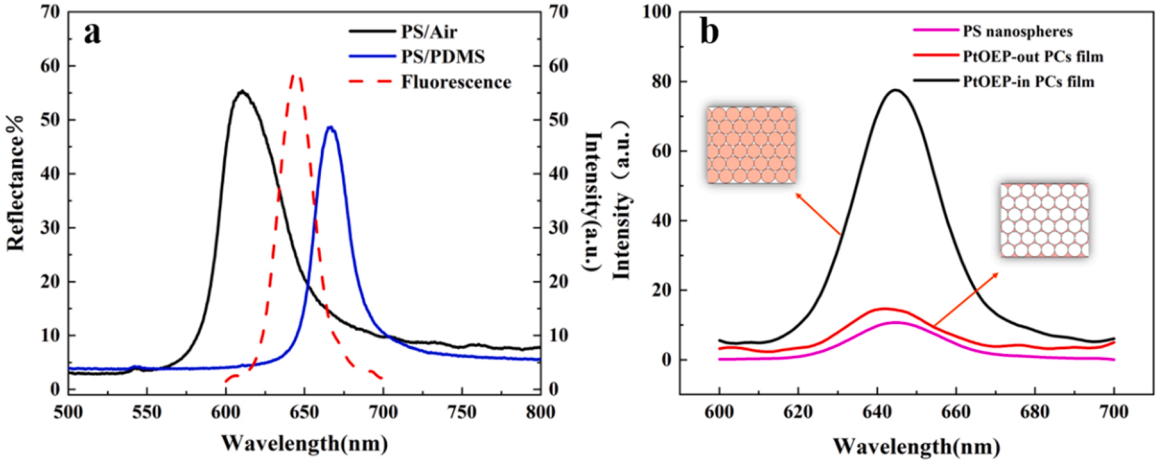

Fig. 2. (a) Reflection spectrum of PS/air PCs (black line) and PS/PDMS PCs (blue line); luminescence emission spectrum of PtOEP (red dotted line); (b) luminescence spectrum of PtOEP-out and PtOEP-in PCs as well as the control group of PtOEP in PS microspheres.

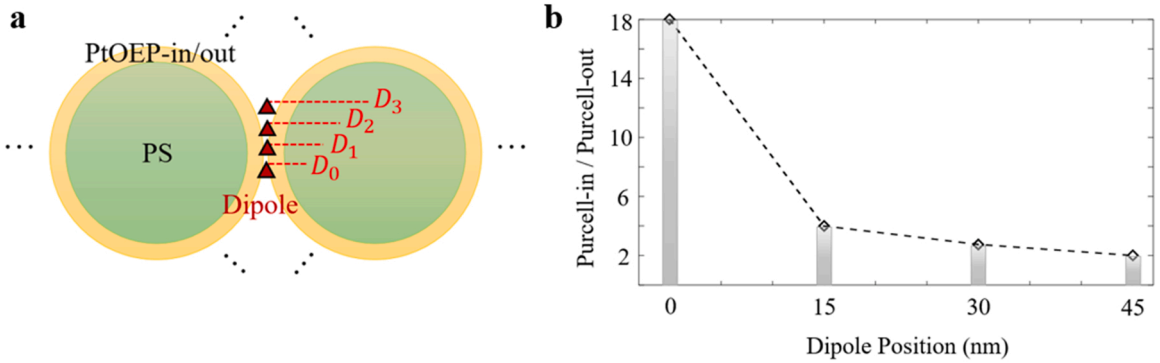

Fig. 4. (a) Schematic of the radiation damping system, where a dipole is placed somewhere between two PS microspheres; (b) Dependence of Purcell enhancement on the dipole position shown in (a) at resonance.

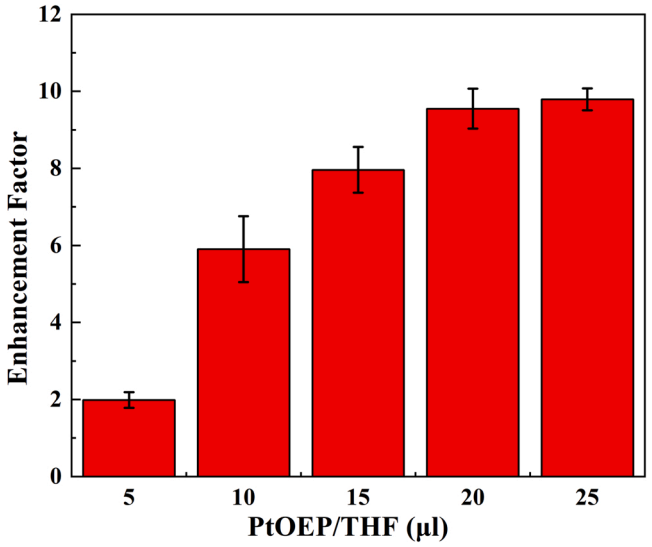

Fig. 5. Enhancement factor of PtOEP-in PCs with different PtOEP volumes.

enhancement of PtOEP-out PCs was achieved when the PtOEP emission light overlapped with the stopband of PCs (Fig. S5). The FL enhancement behaviour observed here is almost consistent with the FDTD numerical simulations for PtOEP-in PCs and PtOEP-out PCs.

3.2. Oxygen-sensing performance of PC FEE-based sensors

To quantify the relation between the luminescence signal I and oxygen content $[O_2]$, the Stern-Volmer equation is employed as follows:

$$\frac{I_0}{I} = 1 + K_{sv}[O_2] \quad (1)$$

where I_0 and I are the luminescence intensities measured in deoxygenated and different oxygenated conditions, respectively. I_0/I is the quenching ratio. K_{sv} is the quenching constant, which indicates the quenching efficiency between oxygen and the OSP. $[O_2]$ is the different oxygen contents in the system. Moreover, the oxygen-sensing sensitivity can be evaluated by K_{sv} and the maximum quenching ratio (I_0/I_{100}), where I_0 and I_{100} are the steady-state PL signals measured in 100% nitrogen (N_2) or 100% oxygen (O_2). The accuracy of the oxygen sensor is illustrated by the linear correlation (R^2).

The typical oxygen sensing of the control group and PC FEE oxygen sensors with PtOEP-in and PtOEP-out PCs was tested. For the control group, there was a low PL intensity of PtOEP with wide luminescence fluctuation; thus, the R^2 was much lower (Fig. S6). In contrast, owing to the FEE of PCs, the luminescence intensity of PtOEP significantly changed with decreasing O_2 (Fig. S7), which showed distinguished resolution and a high signal-to-noise ratio. In detail, the Stern-Volmer equation of the FEE oxygen sensor was fitted during 0%– 21% O_2 and 21%– 100% O_2. Both PtOEP-in and PtOEP-out PC oxygen sensors had R^2 values greater than 0.99 (Fig. 6), demonstrating excellent accuracy compared with earlier studies [49,50]. In particular, the accuracy of the PtOEP-in oxygen sensor was better during 0%– 100% O_2 since a uniform microenvironment was created, preventing self-quenching of PtOEP by the independent PS microspheres. Therefore, the linear relationship (R^2) of the PtOEP-in FEE oxygen sensor was effectively maintained with varying luminescence intensity. The K_{sv} of the PtOEP-in oxygen sensor increased from 8.79 to 10.66 (Figs. 6**a**) and 16.13 (Fig. 6**b**).

In addition, the difference in oxygen sensing was still influenced by the incorporation of PtOEP [32]. The K_{sv} of the PtOEP-out oxygen sensor was increased from 8.79 to 14.22 (Figs. 6**c**) and 16.18 (Fig. 6**d**), where there was a shorter O_2 diffusion channel in the PtOEP-out PC oxygen sensor. Therefore, PtOEP was effectively quenched in the PtOEP-out PC oxygen sensor because PtOEP was outside the PS microspheres.

To facilitate comparison, the improvement in the sensitivity is represented as the relative change in K_{sv}, which is calculated by[14].

$$\Delta = \frac{K_{SV}\text{-}K_{SV}^{ps}}{K_{SV}} \times 100\% = \frac{\Delta K_{SV}}{K_{SV}^{ps}} \times 100\% \quad (2)$$

where Δ is the K_{sv} enhancement efficiency and K_{sv}^{ps} is the Stern-Volmer constant of the control group. The sensitivity enhancement of the PtOEP-in and PtOEP-out oxygen sensors was analysed in dissolved and gaseous oxygen (Table 1). The sensitivity enhancement of the PtOEP-in FEE oxygen sensor was 21.31% and 83.57% and effectively increased with increasing PL intensity since there was a more uniform microenvironment. For the PtOEP-out FEE oxygen sensor, there was strong self-quenching [51], resulting in restrained sensitivity and lower stability.

Notably, considering the extremely high luminescence signal of PtOEP in the hypoxic environment, a 1% filter was used in the experiment. Consequently, the lowest resolution was presumed to lead to inevitable errors for the control group (Fig. S6). Simultaneously, the improvement in oxygen sensing was likely underestimated compared to the performance of PC FEE oxygen sensors in previous studies [52].

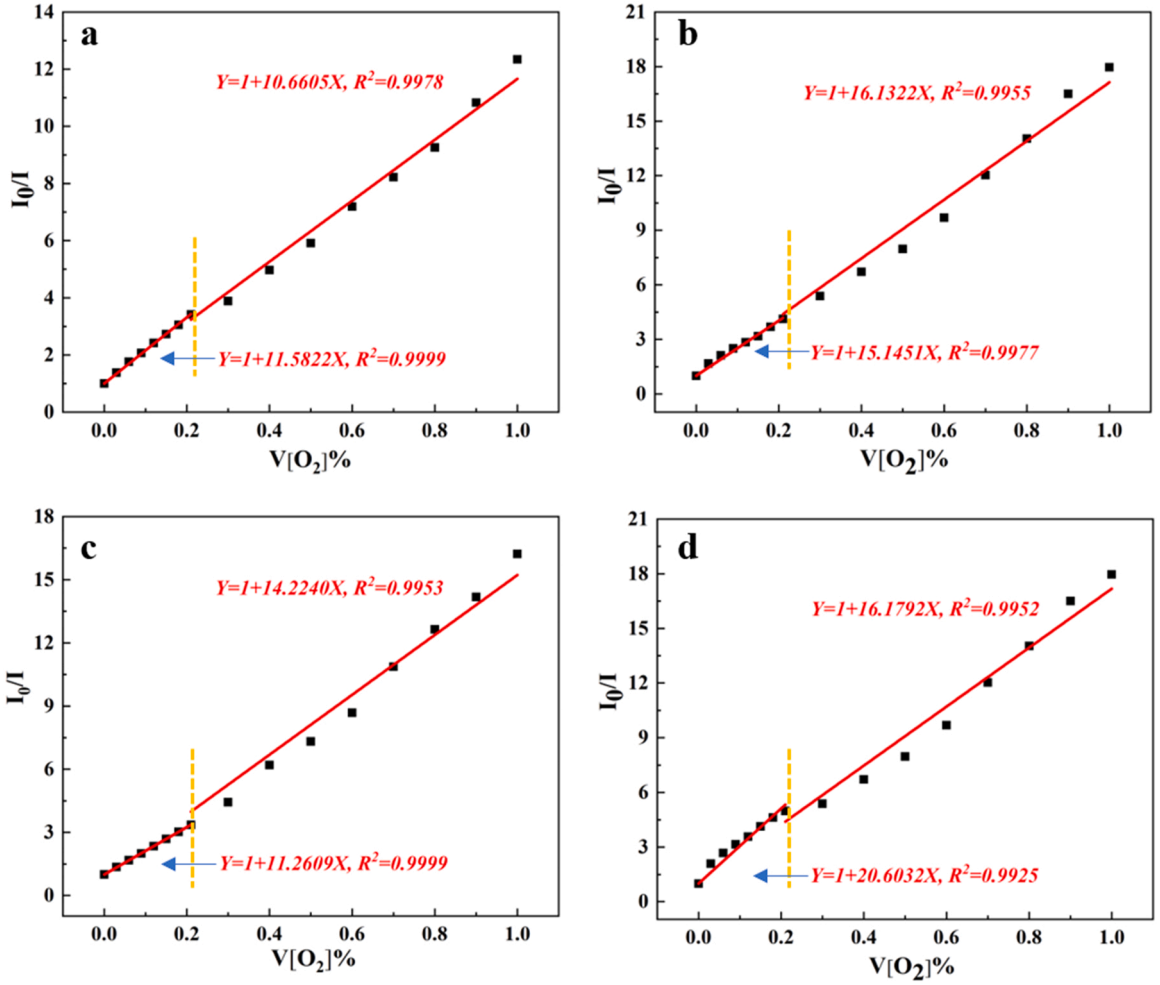

Fig. 6. Typical oxygen sensing of the FEE oxygen sensor in the range of 0%– 100% O_2, PtOEP-in oxygen sensor (a) dissolved oxygen; (b) gaseous oxygen, PtOEP-out oxygen sensor (c) dissolved oxygen; (d) gaseous oxygen.

Table 1
K_{sv} improvement of the PtOEP-in and PtOEP-out oxygen sensors in 0%– 100% O_2.

Sample	Dissolved oxygen		Gaseous oxygen	
	Ksv	$\frac{\Delta Ksv}{Ksv^{ps}} \times 100\%$	Ksv	$\frac{\Delta Ksv}{Ksv^{ps}} \times 100\%$
Control group	8.7880	–	8.7880	–
PtOEP-in	10.6605	21.31%	16.1322	83.57%
PtOEP-out	14.2240	61.86%	16.1792	84.11%

3.3. Optimization of the prepared oxygen sensor

According to previous studies, the embedding rate of PtOEP mainly depends on the THF:H_2O ratio;[53] therefore, the performance of the oxygen sensor is directly affected by the amount of PtOEP/THF. With increasing PtOEP, K_{sv} first increases and then decreases (Fig. 7). When 20 μl of PtOEP was added to the PC FEE oxygen sensor, the optimal oxygen-sensing performance was obtained, which led to the highest sensitivity.

The photostability curves of PtOEP embedded in a different system were tested (Fig. 8). The oxygen sensor with PtOEP-in PCs had the highest luminescence retention rate of 99.11%, which suggests outstanding stability of the FEE oxygen sensor in the long term. Dynamic oxygen sensing was also tested, indicating that the phosphorescence quenching of PtOEP is completely reversible, and the quenching time and recovery time were 76 s and 435 s, respectively (Fig. S8). Thus, a real-time oxygen sensor with high sensitivity and stability was provided, which is promising for gas [54], pH [55], temperature [56], and ion [37] detection based on fluorescent probes.

The relatively bright structural colour of PCs indicated that there is significant potential of PC FEE oxygen sensors for ratiometric oxygen sensing [13]. To show this potential application, fluorescein isothiocyanate (FITC) with emission at 520 nm was introduced as a reference into the above PtOEP-in PC oxygen sensor. Both green and red PL intensities were observed in our PC FEE oxygen sensor (Fig. S9a), indicating that the two dyes FITC and PtOEP swelled into the PS microspheres. The green emission channel (FITC) was assigned as the reference that was insensitive to oxygen. In contrast, the PL signal of the red channel (PtOEP) dynamically responded, varying with different O_2 conditions (Fig. S9b). The xy colour space response of RG sensors was shown over the range of 0%– 100% O_2 (Fig. S10). When the O_2 concentration was increased, the RG sensor colour shifted from orange to green, leading to a high range of the colour space response of the oxygen sensor.

3.4. Flexibility behaviour test of the prepared film

With the development of wearable biosensors for healthcare monitoring [57], flexible oxygen sensor is increasingly required by those with severe asthma or newborns [9], in which researchers are intending to suit the needs of wearers via expanding the functionality of the device [58] or developing high-performance functional materials [59].

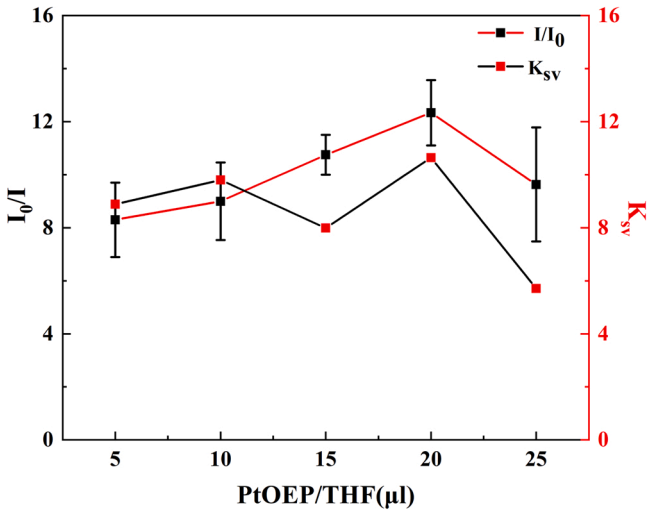

Fig. 7. I_0/I_{100} and K_{sv} changes with the PtOEP/THF volume.

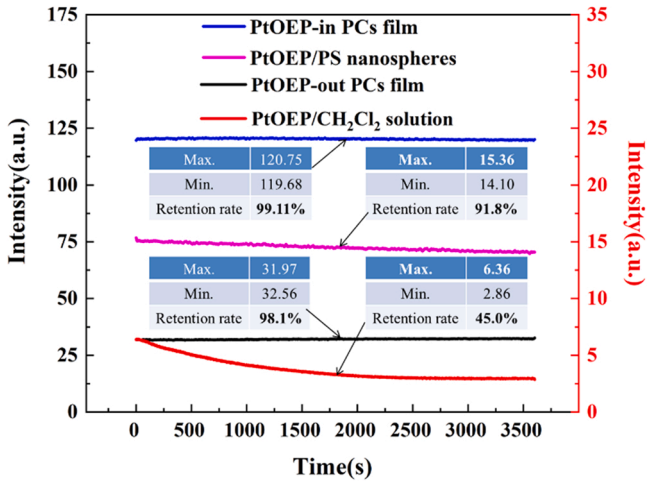

Fig. 8. Photostability curve of PtOEP in different matrices.

Therefore, PDMS was introduced into our PC FEE oxygen sensor to improve the flexibility in this work. Then, the PC FEE oxygen-sensing thin film was tested by bending and stretching, displaying an unchanged distinct structural colour (Fig. 9a). Moreover, the oxygen-sensing thin film can be stretched more than 3 times in length by artificial pulling (Fig. 9b). To further study the flexibility of this oxygen sensor, it was continuously stretched and compressed using a stretching machine (movie S1), and the reflectance of the oxygen-sensing thin film slightly decreased after 100 strain cycles (Fig. S11). In addition, the local microstructure of the middle PCs was characterized by optical microscopy (Fig. S12). Although some microcracks appeared in the sensor platforms, the locally integral microstructure of the PCs was maintained. Therefore, the composite PC FEE oxygen sensor with superior mechanical stability and flexibility is promising for wearable health monitoring.

Supplementary material related to this article can be found online at doi:10.1016/j.addma.2020.101681.

Oxygen sensing before and after stretching was also tested (Fig. S13) to validate the sensor's applicability in wearable health monitoring. The R^2 of the oxygen sensor slightly changed from 0.9973 to 0.9943, and K_{sv} was maintained at 82.68%, illuminating the outstanding mechanical tolerance and high sensitivity of the FEE oxygen sensor in this work.

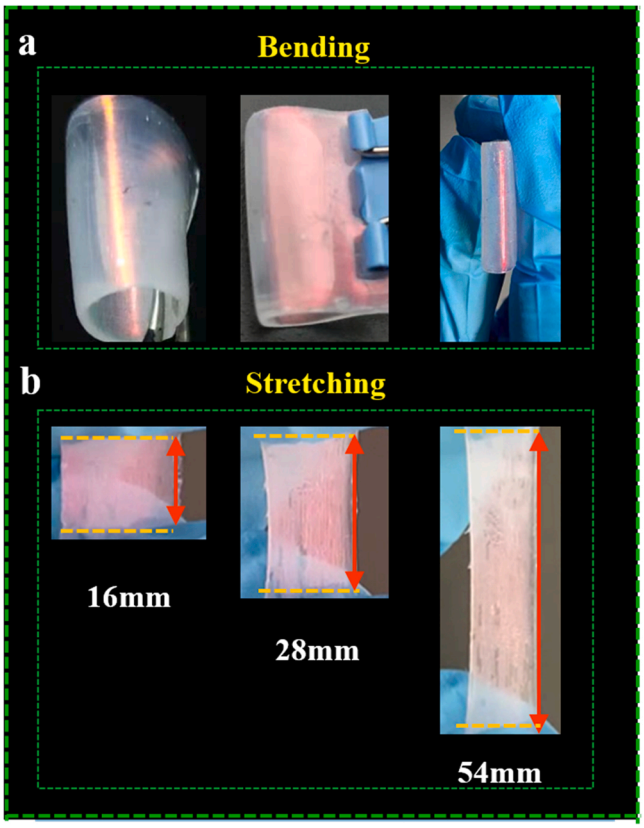

Fig. 9. Flexibility test of a PDM/PS/PDMS PC oxygen-sensing film: (a) bending; (b) stretching.

4. Conclusion

A flexible oxygen sensor based on the PC FEE was prepared, and high sensitivity, accuracy, and stability in oxygen sensing were achieved due to the enhanced PL intensity of PtOEP. The flexible oxygen sensor was mainly composed of two layers of thin PDMS and a layer of monolithic PS PCs embedded in PtOEP. Two different oxygen sensors with PtOEP-in or PtOEP-out PCs were studied in terms of FEE and oxygen sensing, showing that the enhancement factor was more than 12-fold compared to the control group (disorderly PS microspheres). Simultaneously, the sensitivity of the PtOEP-in (K_{sv}=16.13) and PtOEP-out (K_{sv}=16.18) sensors was significantly improved because of the FEE when the photonic bandgap of the PCs partially overlapped with the emission peak of PtOEP. The increased LDOS around the PC gaps was responsible for the enhanced PL. Interestingly, there was a more uniform and independent microenvironment in the PtOEP-in oxygen sensor, which led to higher stability and accuracy in oxygen sensing. Moreover, satisfactory anti-photobleaching (luminescence retention rate>99%) was exhibited, illustrating that PtOEP leakage was effectively prevented by combining PS microspheres with PDMS as a matrix material. Finally, excellent flexibility and stability were revealed by bending and stretching, displaying slight changes in reflectance and microstructure. Therefore, a high-sensitivity oxygen sensor is provided using the FEE of PCs in wound sensing and wearable health monitoring.

CRediT authorship contribution statement

Sai Chen: Conceptualization, Investigation, Methodology, Validation, Visualization, Writing – original draft, Writing – review & editing. **Qun Ren**: Investigation, Writing – review & editing. **Ke Zhang**: Conceptualization, Methodology, Funding acquisition, Supervision , Writing – review & editing. **Wei E. I. Sha**: Formal analysis, Validation.

Tingting Hao: Conceptualization, Methodology, Validation. **Hongbo Xu**: Visualization, Validation. **Jiupeng Zhao**: Conceptualization, Supervision, Writing – review & editing. **Yao Li**: Methodology, Supervision, Writing – review & editing.

Declaration of Competing Interest

The authors declare that they have no known competing financial interests or personal relationships that could have appeared to influence the work reported in this paper.

Acknowledgements

This work was partially supported by the National Natural Science Foundation of China (51603056), the Excellent Youth Foundation of Heilongjiang Province of China (YQ2019E020), and the EU Horizon 2020 Marie Skłodowska-Curie Actions Individual Fellowships (MSCA-IF 658478).

Appendix A. Supporting information

Supplementary data associated with this article can be found in the online version at doi:10.1016/j.snb.2021.131326.

References

[1] H. Shi, X. Ma, Q. Zhao, B. Liu, Q. Qu, Z. An, Ultrasmall phosphorescent polymer dots for ratiometric oxygen sensing and photodynamic cancer therapy, Adv. Funct. Mater. 24 (2014) 4823–4830.
[2] Z. Lv, L. Zou, H. Wei, S. Liu, W. Huang, Q. Zhao, Phosphorescent starburst Pt(II) porphyrins as bifunctional therapeutic agents for tumor hypoxia imaging and photodynamic therapy, ACS Appl. Mater. Interfaces 10 (2018) 19523–19533.
[3] Z. Li, H. Marks, C.L. Evans, G. Apiou-Sbirlea, Sensing, monitoring, and release of therapeutics: the translational journey of next generation bandages, J. Biomed. Opt. 24 (2019) 1–9.
[4] H.P. Misra, I. Fridovich, A convenient calibration of the clark oxygen electrode, analytical biochemistry, Anal. Biochem. 70 (1976) 632–634.
[5] X.-d Wang, O.S. Wolfbeis, Optical methods for sensing and imaging oxygen: materials, spectroscopies and applications, Chem. Soc. Rev. 43 (2014) 3666–3761.
[6] Z. Zhou, R. Shinar, A.J. Allison, J. Shinar, Enhanced photoluminescence of oxygen sensing films through doping with high dielectric constant particles, Adv. Funct. Mater. 17 (2007) 3530–3537.
[7] E. Roussakis, Z.X. Li, A.J. Nichols, C.L. Evans, Oxygen-sensing methods in biomedicine from the macroscale to the microscale, Angew. Chem. -Int. Ed. 54 (2015) 8340–8362.
[8] Y. Yao, X. Liu, Y. Shao, Y. Ying, J. Ping, Noble metal alloy nanoparticles coated flexible MoS_2 paper for the determination of reactive oxygen species, Biosens. Bioelectron. 166 (2020), 112463.
[9] M. Ochoa, R. Rahimi, J. Zhou, H. Jiang, C.K. Yoon, D. Maddipatla, B.B. Narakathu, V. Jain, M.M. Oscai, T.J. Morken, R.H. Oliveira, G.L. Campana, O.W. Cummings, M.A. Zieger, R. Sood, M.Z. Atashbar, B. Ziaie, Integrated sensing and delivery of oxygen for next-generation smart wound dressings, Microsyst. Nanoeng. 6 (2020) 46.
[10] J.N. Demas, B.A. DeGraff, P.B. Coleman, Oxygen sensors based on luminescence quenching, Anal. Chem. 71 (1999) 793A–800A.
[11] P. Henke, K. Kirakci, P. Kubat, M. Fraiberk, J. Forstova, J. Mosinger, Antibacterial, antiviral, and oxygen-sensing nanoparticles prepared from electrospun materials, ACS Appl. Mater. Interfaces 8 (2016) 25127–25136.
[12] R.-F. Wang, H.-Q. Peng, P.-Z. Chen, L.-Y. Niu, J.-F. Gao, L.-Z. Wu, A hydrogen-bonded-supramolecular-polymer-based nanoprobe for ratiometric oxygen sensing in living cells, Adv. Funct. Mater. 26 (2016) 5419–5425.
[13] S.M. Borisov, R. Fischer, R. Saf, I. Klimant, Exceptional oxygen sensing properties of new blue light-excitable highly luminescent Europium(III) and Gadolinium(III) complexes, Adv. Funct. Mater. 24 (2014) 6548–6560.
[14] S. Lee, J.-W. Park, Luminescent oxygen sensors with highly improved sensitivity based on a porous sensing film with increased oxygen accessibility and, photoluminescence, Sens. Actuators B Chem. 249 (2017) 364–377.
[15] Y. Mao, Z. Mei, J. Wen, G. Li, Y. Tian, B. Zhou, Y. Tian, Honeycomb structured porous films from a platinum porphyrin-grafted poly(styrene-co-4-vinylpyridine) copolymer as an optical oxygen sensor, Sens. Actuators B Chem. 257 (2018) 944–953.
[16] A. Li, H. Liu, P. Ouyang, P.-H. Yang, H.-H. Cai, J. Cai, A sensitive probe for detecting intracellular reactive oxygen species via glutathione-mediated nanoaggregates to enhance Resonance Rayleigh scattering signals, Sens. Actuators B Chem. 246 (2017) 190–196.
[17] C.-J. Lim, J.-W. Park, Luminescent oxygen-sensing films with improved sensitivity based on light scattering by TiO_2 particles, Sens. Actuators B Chem. 253 (2017) 934–941.
[18] Q. Zhang, D. Myers, J. Lan, S.A. Jenekhe, G. Cao, Applications of light scattering in dye-sensitized solar cells, Phys. Chem. Chem. Phys. 14 (2012) 14982–14998.
[19] H. Kang, J.-S. Lee, W.S. Chang, S.-H. Kim, Liquid-impermeable inverse opals with invariant photonic bandgap, Adv. Mater. 27 (2015) 1282–1287.
[20] J.-Y. Shieh, J.-Y. Kuo, H.-P. Weng, H.H. Yu, Preparation and evaluation of the bioinspired ps/pdms photochromic films by the self-assembly dip-drawing method, Langmuir 29 (2013) 667–672.
[21] H. Wang, M. Li, Z. Yin, T. Zhang, X. Chen, D. Zhou, Remarkable enhancement of upconversion luminescence on CapAg/PMMA ordered platform and trademark anticounterfeiting, ACS Appl. Mater. Interfaces 9 (2017) 37128–37135.
[22] B. Gao, L. Tang, D. Zhang, Z. Xie, E. Su, H. Liu, Transpiration-inspired fabrication of opal capillary with multiple heterostructures for multiplex aptamer-based fluorescent assays, ACS Appl. Mater. Interfaces 9 (2017) 32577–32582.
[23] E. Yablonovitch, R. Bhat, J.P. Harbison, R.A. Logan, Survey of defect-mediated recombination lifetimes in GaAs epilayers grown by different methods, Appl. Phys. Lett. 50 (1987) 1197–1199.
[24] C.-H. Hsieh, Y.-C. Lu, H. Yang, Self-assembled mechanochromic shape memory photonic crystals by doctor blade coating, ACS Appl. Mater. Interfaces 12 (2020) 36478–36484.
[25] S.H. Park, Y.N. Xia, Assembly of mesoscale particles over large areas and its application in fabricating tunable optical filters, Langmuir 15 (1999) 266–273.
[26] Z. Meng, S. Wu, B. Tang, W. Ma, S. Zhang, Structurally colored polymer films with narrow stop band, high angle-dependence and good mechanical robustness for trademark anti-counterfeiting, Nanoscale 10 (2018) 14755–14762.
[27] Y. Liu, H. Wang, J. Ho, R.C. Ng, R.J.H. Ng, V.H. Hall-Chen, Structural color three-dimensional printing by shrinking photonic crystals, Nat. Commun. 10 (2019) 4340.
[28] X. Fei, T. Lu, J. Ma, W. Wang, S. Zhu, D. Zhang, Bioinspired polymeric photonic crystals for high cycling ph-sensing performance, ACS Appl. Mater. Interfaces 8 (2016) 27091–27098.
[29] H. Li, J. Wang, F. Liu, Y. Song, R. Wang, Fluorescence enhancement by heterostructure colloidal photonic crystals with dual stopbands, J. Colloid Interface Sci. 356 (2011) 63–68.
[30] L. Zhang, J. Wang, S. Tao, C. Geng, Q. Yan, Universal fluorescence enhancement substrate based on multiple heterostructure photonic crystal with super-wide stopband and highly sensitive Cr(VI) detecting performance, Adv. Opt. Mater. 6 (2018) 1701344–1702784.
[31] A. Pokhriyal, M. Lu, C.S. Huang, S. Schulz, B.T. Cunningham, Multicolor fluorescence enhancement from a photonics crystal surface, Appl. Phys. Lett. 97 (2010), 121108.
[32] E. Eftekhari, I.S. Cole, Q. Li, The effect of fluorophore incorporation on fluorescence enhancement in colloidal photonic crystals, Phys. Chem. Chem. Phys. 18 (2016) 1743–1749.
[33] G. Chen, D. Wang, W. Hong, L. Sun, Y. Zhu, X. Chen, Fluorescence enhancement on large area self-assembled plasmonic-D-3 photonic crystals, Small 13 (2017), 1602612.
[34] E. Eftekhari, P. Broisson, N. Aravindakshan, Z. Wu, I.S. Cole, X. Li, Sandwich-structured TiO_2 inverse opal circulates slow photons for tremendous improvement in solar energy conversion efficiency, J. Mater. Chem. A 5 (2017) 12803–12810.
[35] M. Li, F. He, Q. Liao, J. Liu, L. Xu, L. Jiang, Ultrasensitive DNA detection using photonic crystals, Angew. Chem. -Int. Ed. 47 (2008) 7258–7262.
[36] J. Hou, H. Zhang, Q. Yang, M. Li, Y. Song, L. Jiang, Bio-inspired photonic-crystal microchip for fluorescent ultratrace detection, Angew. Chem. -Int. Ed. 53 (2014) 5791–5795.
[37] Y. Huang, F. Li, M. Qin, L. Jiang, Y. Song, A multi-stopband photonic-crystal microchip for high-performance metal-ion recognition based on fluorescent detection, Angew. Chem. -Int. Ed. 52 (2013) 7296–7299.
[38] P. Lova, S. Congiu, K. Sparnacci, A. Angelini, L. Boarino, M. Laus, Core-shell silica-rhodamine B nanosphere for synthetic opals: from fluorescence spectral redistribution to sensing, RSC Adv. 10 (2020) 14958–14964.
[39] J. Chi, C. Shao, X. Du, H. Liu, Z. Gu, Generating microdroplet array on photonic pseudo-paper for absolute quantification of nucleic acids, ACS Appl. Mater. Interfaces 10 (2018) 39144–39150.
[40] X. Lu, R. Li, B. Han, H. Ma, X. Hou, Y. Kang, Fluorescence sensing of formaldehyde and acetaldehyde based on responsive inverse opal photonic crystals: a multiple-application detection platform, ACS Appl. Mater. Interfaces 13 (2021) 13792–13801.
[41] Z. Xie, K. Cao, Y. Zhao, L. Bai, H. Gu, H. Xu, An optical nose chip based on mesoporous colloidal photonic crystal beads, Adv. Mater. 26 (2014) 2413–2418.
[42] A. Goodall, M. Wilkinson, J. Hearn, Mechanism of emulsion polymerization of styrene in soap-free systems, J. Polym. Sci.: Polym. Chem. Ed. 15 (1977) 2193–2218.
[43] Z.C. Zhou, X.S. Zhao, Opal and inverse opal fabricated with a flow-controlled vertical deposition method, Langmuir 21 (2005) 4717–4723.
[44] K. Zhang, H. Zhang, Y. Wang, Y. Tian, J. Zhao, Y. Li, High sensitivity and accuracy dissolved oxygen (DO) detection by using PtOEP/poly(MMA-co-TFEMA) sensing film, Spectrochim. Acta Part a-Mol. Biomol. Spectrosc. 170 (2017) 242–246.
[45] Y.-Q. Zhang, J.-X. Wang, Z.-Y. Ji, W.-P. Hu, L. Jiang, Y.-L. Song, Solid-state fluorescence enhancement of organic dyes by photonic crystals, J. Mater. Chem. 17 (2007) 90–94.
[46] W.B. Connick, D. Geiger, R. Eisenberg, Excited-state self-quenching reactions of square planar platinum(II) diimine complexes in room-temperature fluid solution, Inorg. Chem. 38 (1999) 3264–3265.
[47] N. Sultanova, S. Kasarova, I. Nikolov, Dispersion properties of optical polymers, Acta Phys. Pol. A 116 (2009) 585–587.

[48] A. Abuelwafa, A. El-Denglawey, M. Dongol, M. El-Nahass, T. Soga, Structural and optical properties of nanocrystalline platinum octaethylporphyrin (PtOEP) thin films, J. Alloy. Compd. 15 (2015) 415–422.
[49] R. Xue, P. Behera, J. Xu, M.S. Viapiano, J.J. Lannutti, Polydimethylsiloxane core-polycaprolactone shell nanofibers as biocompatible, real-time oxygen sensors, Sens. Actuators B Chem. 192 (2014) 697–707.
[50] N. Shehata, I. Kandas, E. Samir, In-situ gold-ceria nanoparticles: superior optical fluorescence quenching sensor for dissolved oxygen, Nanomaterials 10 (2020) 314.
[51] W. Connick, D. Geiger, R. Eisenberg, Excited-state self-quenching reactions of square planar Platinum(II) diimine complexes in room-temperature fluid solution, Inorg. Chem. 38 (1999) 3264–3265.
[52] K. Zhang, L. Luo, W. Li, H. Zhang, Y. Zhang, J. Zhao, High-performance dissolved oxygen sensors based on Platinum(II) porphyrin embedded in polystyrene beads, N. J. Chem. 41 (2017) 6646–6652.
[53] T. Behnke, C. Wuerth, K. Hoffmann, M. Huebner, U. Panne, U. Resch-Genger, Encapsulation of hydrophobic dyes in polystyrene micro- and nanoparticles via swelling procedures, J. Fluoresc. 21 (2011) 937–944.
[54] Y. Qi, L. Chu, W. Niu, B. Tang, S. Wu, W. Ma, New encryption strategy of photonic crystals with bilayer inverse heterostructure guided from transparency response, Adv. Funct. Mater. 29 (2019), 1903743.
[55] S. Schreml, R.J. Meier, O.S. Wolfbeis, M. Landthaler, R.-M. Szeimies, P. Babilas, 2D luminescence imaging of pH in vivo, Proc. Natl. Acad. Sci. USA 108 (2011) 2432–2437.
[56] M.I.J. Stich, S. Nagl, O.S. Wolfbeis, U. Henne, M. Schaeferling, A dual luminescent sensor material for simultaneous imaging of pressure and temperature on surfaces, Adv. Funct. Mater. 18 (2008) 1399–1406.
[57] X.-L. Qi, S.-Y. Liu, R.-B. Lin, P.-Q. Liao, J.-W. Ye, Z. Lai, Phosphorescence doping in a flexible ultramicroporous framework for high and tunable oxygen sensing efficiency, Chem. Commun. 49 (2013) 6864–6866.
[58] J. Jeong, M. Essafi, C. Lee, M. Haoues, M.F. Diouani, H. Kim, Ultrasensitive detection of hazardous reactive oxygen species using flexible organic transistors with polyphenol-embedded conjugated polymer sensing layers, J. Hazard. Mater. 355 (2018) 17–24.
[59] Y. Lei, W. Zhao, Y. Zhang, Q. Jiang, J.-H. He, A. Baeumner, A mxene-based wearable biosensor system for high-performance in vitro perspiration analysis, Small 15 (2019), 1901190.

Sai Chen is currently working toward a Ph.D. degree in the School of Chemistry and Chemical Engineering, Harbin Institute of Technology.

Qun Ren received her Ph.D. degree in the Department of Electronic and Electrical Engineering from University College London in 2019. Now she is a lecturer in the School of Electrical and Information Engineering at Tianjin University. Her research interests are plasmonic sensing, nanophotonics and metasurfaces for sensor applications.

Ke Zhang received her Ph.D. degree (2011) in Polymer Science and Engineering from Inha University, Korea. From 2015–2017, she worked at Queen Mary University of London as a Marie-Curie Individual Fellow. She is currently an associate professor at the School of Chemistry and Chemical Engineering, Harbin Institute of Technology. Her current research focuses on synthesis and application of optical-based sensors, polymer nanocomposite, polymer and suspension rheology, electrorheology and magnetorheology.

Wei E.I. Sha received B.S. and Ph.D. degrees in Electronic Engineering at Anhui University, Hefei, China, in 2003 and 2008, respectively. From 2008–2017, he was a Postdoctoral Research Fellow and then a Research Assistant Professor in the Department of Electrical and Electronic Engineering at the University of Hong Kong, Hong Kong. From 2018–2019, he worked at University College London as a Marie-Curie Individual Fellow. From 2017, he joined the College of Information Science & Electronic Engineering at Zhejiang University, Hangzhou, China, where he is currently a tenure-tracked Assistant Professor. His research interests include theoretical and computational research in electromagnetics and optics, focusing on multiphysics and interdisciplinary research. His research involves fundamental and applied aspects in computational and applied electromagnetics, nonlinear and quantum electromagnetics, micro- and nano-optics, optoelectronic device simulation, and multiphysics modeling.

Tingting Hao is about to receive her Ph.D. degree from the School of Chemistry and Chemical Engineering, Harbin Institute of Technology in 2021.

Hongbo Xu is currently an associate professor in the School of Chemistry and Chemical Engineering, Harbin Institute of Technology. He received his Ph.D. degree (2011) from the College of Chemistry, Jilin University. His current research focuses on biomimetic optical and thermal materials with micro/ nanoscale hierarchical structures, optical surfaces in nature, and biomimetic optical device design and fabrication.

Jiu Peng Zhao received her Ph.D. degree from Harbin Institute of Technology (HIT) in 2000. She has been a Professor in the School of Chemical Engineering and Technology at HIT since 2007. Her research is focusing on the design and fabrication of nanostructured materials for energy storage applications and electrical devices.

Yao Li has been a Professor of Materials Science in Harbin Institute of Technology (HIT) since 2005 and leads the laboratory of Functional Composite Materials in Center for Composite Materials. His research interests include fabrication and engineering nanostructured inorganic materials and polymers with well-defined microstructure and multiple length scales, and their applications for energy storage, and electrochromism. He is the author or co-author of over 120 papers, 62 patents, and 3 books in the fields of materials science and processing. He was selected as “The Yangtze River scholar Professor” by Ministry of Education, New Century Excellent Talents program” and “Distinguished Young Scholars for Heilongjiang Province” and “Youth leader in Science and Technology Innovation” by Ministry of Science and Technology. He was awarded “Science and Technology Award for the Youth of China”, “National Award of the outstanding Scientific and Technological Workers” and “the first Prize of Natural Science of Heilongjiang Province”. He is the council member of Chinese Materials Research Society and Functional Materials Society of China.